Int. J. Electrochem. Sci., 17 **(2022)** Article Number: 221156, doi: 10.20964/2022.11.58

International Journal of
ELECTROCHEMICAL
SCIENCE
www.electrochemsci.org

Analytical Solution for One-dimensional Electro-osmosis Consolidation of Low Permeability Soil in the Recessed Chamber Filter Press

Chengwei Yin, Bing Liang, Liguo Jiang, Weiji Sun, Chengyu Yin

School of Mechanics & Engineering, Liaoning Technical University, Fuxin, Liaoning Province, 123000, China
E-mail: princell@163.com

Received: 18 August 2022 / *Accepted:* 2 October 2022 / *Published:* 10 October 2022

In this work, established a one-dimensional mathematical model to describe the electro-osmosis dewatering process of the filter cake in the recessed chamber filter (RCF) press chamber. Based on the consolidation theory in geotechnical engineering, analytical solutions with an initial parabolic distribution of the pore water pressure and the average degree of consolidation were derived, the effectiveness of which was further verified by laboratory tests. The analytical results indicate that the impact of the ratio of the negative pore water pressure at the anode to the maximum initial pore water pressure is significant on the electro-osmosis dewatering of the filter cake. By comparison with the verification experimental results, it reveals that the proposed analytical solutions could help design electro-osmotically enhanced systems in the RCF press.

Keywords: electro-osmosis; recessed chamber filter press; analytical solution; non-linear initial condition

1. INTRODUCTION

Extraction or recovery of water in fine-grained soil represents a significant research topic in geotechnical engineering, such as the treatment of mud in drilling and shield tunnelling, the disposal of dredged sediments, and so on. A wide range of technologies could separate liquid from the solid phase. Nevertheless, a significant amount of water remains trapped in fine-grained particles owing to the high amount of internal nano-scale capillaries [1, 2]. Although mechanical dewatering is widely used in geotechnical engineering [3]. The filtered materials containing a large number of fine-grained particles l dewatering often have very low hydraulic permeability (<10-7 cm/s). This implies that mechanical dewatering is not efficient enough because trapped water moves quite slowly even when a very high pressure is applied [4].

Water in porous materials can be divided into four types: bulk water, capillary water, vicinal water, and intracellular water [5]. Conventional mechanical dewatering techniques could effectively remove bulk water but have difficulty mobilizing vicinal water. Generally, as most solid particles involved in geotechnical engineering are negatively charged, they are surrounded by a layer with a higher density of positive charges, forming the electric double layer. Thus, electro-osmosis has the potential to remove free, interstitial, and vicinal water [6]. Therefore, combing the electro-osmosis technique with mechanical pressure could improve the dewatering drastically, both in dewatering rate and final solid content [7-9].

For mechanical dewatering processes, filter presses, filter belt presses, rotary drum filters, and decanter centrifuges are widely used among various dewatering devices. Previous researchers have demonstrated the successful use of electro-osmosis dewatering in conjunction with belt filter presses [4, 5, 10-12] and filter presses or diaphragm filter presses [8, 9, 13] at the laboratory, pilot, and industrial scales. Most published theoretical studies focus on belt filter presses and diaphragm filter presses, even though the recessed chamber filter press (RCF press) is recognized as the most efficient liquid/solids separation device for dewatering and filtration.

The modelling of electro-osmotically enhanced mechanical pressure dewatering has been a matter of interest for decades, and many theoretical analysis methods and corresponding solution schemes have been proposed [14]. Since the electro-osmosis dewatering of filter materials could be considered a consolidation process [15], most existing theoretical models are based on the classical consolidation theory in geotechnical engineering [16-21]. The processes of the solid-liquid separation in filter press include filtration and expression. According to the application process of electro-osmosis in the RCF press described by Kondoh and Hiraoka [13], a D.C. electric field is applied at a predetermined time after filtration starts. This indicates that the initial condition of the electro-osmosis varies with operating conditions. For most filter press processes combined with electro-osmosis technology, the electric field is commonly applied at the end of the filtration. Meanwhile, owing to the pressure applied during the filtration and expression periods of the RCF press being constant, most previous studies have derived the analytical solutions of the electro-osmosis consolidation models with the assumption of the uniform initial condition [22]. Although some studies concerning the filtration process in RCF press suggest that the filter cake's porosity and pore water pressure have a non-linear distribution [21], there have been few investigations into the response of non-uniform initial pore water pressure to the electro-osmosis dewatering performance.

The paper aims to develop a one-dimensional mathematical model to describe the electro-osmosis dewatering process of the filter cake in the RCF press chamber based on classical Terzaghi consolidation theory and to derive analytical solutions under the following three conditions: (1) electro-osmosis starts at the end of the filtration period, *i.e.* the RCF press chamber is filled with filter materials; (2) the pore water pressure in the filter cake has a parabolic distribution at the beginning of the electro-osmosis; and (3) the RCF press does not have a diaphragm, *i.e.* there is no pressing process during the electro-osmosis. This work will contribute to a deeper understanding of the electro-osmosis dewatering process of the filter cake in the RCF press chamber and may assist in optimizing the operation of electro-osmosis dewatering in the RCF press. This paper will use electro-osmosis consolidation to refer to electro-osmosis dewatering.

2. THEORETICAL ANALYSIS

2.1 Overview of the electro-osmosis in the RCF press

A schematic representation of one-dimensional electro-osmotic consolidation in the RCF press is illustrated in **Fig. 1,** derived from the model proposed by Kondoh and Hiraoka [13]. Generally, the slurry is pumped into the filter press, and the solids are distributed evenly in each chamber. Most of the solid/liquid separation is accomplished by the particulates building on the cloth, and the solid begins to form a layer on the cloth. This layer traps the fine particles and eventually forms a filter cake. The filter cake then becomes a depth filter as the dewatering process continues. The filtrate (liquid) usually leaves the filter pack (plates) through corner ports into a manifold. Once the chambers are full, the filling process is complete. Then a D.C. electric field is applied to initiate the electro-osmosis consolidation. According to the procedures mentioned above, it is possible to develop a one-dimensional electro-osmosis consolidation model along the direction of the filter cake thickness (see **Fig. 1**). For each chamber, the left electrode is the anode, which is impenetrable to solid and liquid. On the right side is the cathode, which is set to be open and accessible to water flow. A constant electrical potential is applied between the electrodes, indicating the voltage at the anode (V_{anode}).

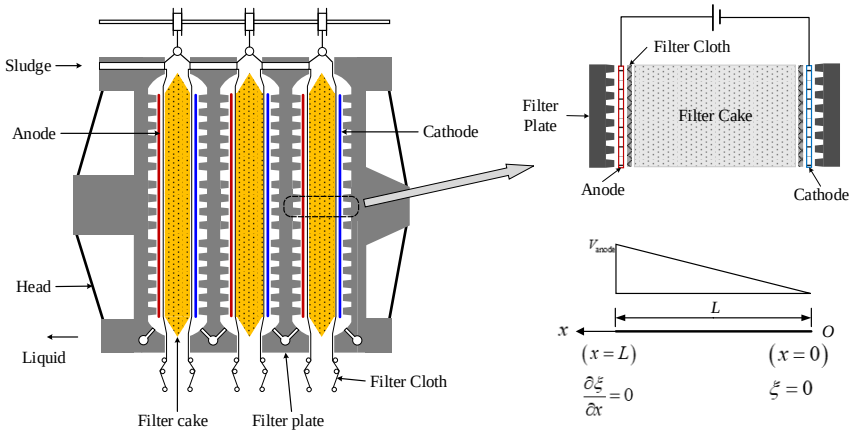

Figure 1. Schematic diagram of the electro-osmosis in the RCF press chamber.

2.2 Basic hypotheses

The following assumptions were made to develop the analytical model for electro-osmotic consolidation of compressible filter cakes. Most of them are based on the hypotheses proposed by Esrig [23]: (1) The filter cake is homogeneous under the fully saturated condition, and the electrical properties of the filter cake keep constant over time. (2) The physical-chemical properties of the filter cake are uniform and constant with time. (3) The electric field is applied after the filling process, which is economically favourable. (4) The velocity of pore water flow due to electro-osmosis is proportional to the electrical gradient and can be superimposed linearly to the hydraulic gradient. (5) All electrical energy is used to drive the movement of the pore water, *i.e.*, the electrolytic reaction of the electrodes is

not considered. (6) The voltage applied across the filter cake maintains constant, *i.e.*, the interface effect between the filter cake and electrodes is neglected.

2.3 Mass balance equations of the pore water

For one-dimensional consolidation in a uniform porous media, the mass balance of pore water for a volume element of the filter cake yields:

$$\frac{1}{1+e}\frac{\partial e}{\partial t}=\frac{\partial}{\partial x}\left(\frac{k_{\mathrm{h}}}{\gamma_{\mathrm{w}}}\frac{\partial u}{\partial x}+k_{\mathrm{e}}\frac{dV}{dx}\right) \quad (1)$$

where e is the local void ratio of the filter cake, dimensionless. k_{e} is the electro-osmotic permeability coefficient, $m^2/(V\cdot s)$. x is the distance from the cathode, m. V is the local voltage at x, Volt. dV/dx is the voltage gradient, V/m. k_{h} is the hydraulic permeability, m/s. γ_w is the unit weight of water, N/kg. u is the excess pore water pressure in the filter cake, Pa, which is a function of the coordinate x and time t, Pa. $\partial u/\partial x$ is the hydraulic pressure gradient, Pa/m. According to Terzarghi's effective stress theory, the increase in effective stress results from the decrease of excess pore water pressure, *i.e.* $\partial\sigma'=-\partial u$. The change in the void ratio (∂e) is due to the increase of effective stress ($\partial\sigma'$); assuming that they are linearly related, then

$$\partial e=-\alpha_v\partial\sigma'=\alpha_v\partial u \quad (2)$$

α_v is the coefficient of compressibility of the filter cake, $Pa^{-1,}$ which could be considered as a constant parameter within a range of σ'.

2.4 Basic equation of the electro-osmosis consolidation

The basic equation which controls the progress of the electro-osmotic consolidation of the filter cake is

$$m_v\frac{\partial u}{\partial t}=\frac{\partial}{\partial x}\left(\frac{k_{\mathrm{h}}}{\gamma_{\mathrm{w}}}\frac{\partial u}{\partial x}+k_{\mathrm{e}}\frac{dV}{dx}\right) \quad (3)$$

where $m_v=\alpha_v/(1+e)$ is the coefficient of volume compressibility of the filter cake, Pa^{-1}. By introducing a dummy variable ξ named by Esrig [23]

$$\xi=\frac{k_e}{k_h}\gamma_w V(x,t)+u(x,t) \quad (4)$$

Eq. 3 could be transformed into

$$c_v\frac{\partial^2\xi}{\partial x^2}=\frac{\partial\xi}{\partial t} \quad (5)$$

where $c_v=k_{\mathrm{h}}/m_v\gamma_{\mathrm{w}}$ is the Terzaghi coefficient of consolidation, m^2/s. **Eq. 5** is a linear and homogeneous partial differential equation that could be solved under appropriate boundaries and initial conditions.

2.5 Boundary conditions

The boundary conditions are when the fluid velocity equals zero at the anode, and the pore pressure equals zero at the cathode (see **Fig.1**):

Cathode (drained): $x=0$, $0<t<\infty$; $V=0$, $u=0$; $\xi=0$ (6)

Anode (undrained): $x=L$, $0<t<\infty$, $\frac{\partial \xi}{\partial x}=0$ (7)

where L is the distance between the cathode and the anode.

2.6 Initial condition

At the end of the filtration process, the excess pore water pressure within the filter cake may be an initial non-linear distribution. Tiller and Horng [21] pointed out that the excess pore water pressure reaches the maximum at feed and zero on either side. To simplify the analysis, we assume that the initial pore water pressure has a parabolic distribution throughout the filter cake:

$$u_{\text{initial}}=a+bx+cx^2 \quad (8)$$

where a (Pa), b (Pa/m), and c (Pa/m^2) are empirical coefficients and x is the distance from the cathode. To satisfy the boundary conditions $u=0$ at $x=0$ and $x=L$, the coefficient a must be zero and the coefficient $b=-cL$. Meanwhile, $u=u_{\text{applied}}$ should also be satisfied $x=L/2$, which leads to the coefficient $b=4u_{\text{applied}}$. Here, u_{applied} (Pa) is the pore water pressure delivered by the pump at the end of the filling period, which could be considered as the maximum pore water pressure within the filter cake at the end of the constant pressure filtration. Therefore, the initial condition could be written as follows:

$$u_{\text{initial}}=-4u_{\text{applied}}\left[\left(\frac{x}{L}\right)^2-\left(\frac{x}{L}\right)\right] \quad (x=x,\ t=0) \quad (9)$$

and

$$\xi=-4u_{\text{applied}}\left[\left(\frac{x}{L}\right)^2-\left(\frac{x}{L}\right)\right]+\frac{k_{\text{e}}\gamma_{\text{w}}}{k_{\text{h}}}V(x) \quad (10)$$

The value of u_{applied} depends on the characteristic curve and the feed pressure of the feed pump u_{feed}. When $u_{\text{applied}}=0$, the solution of **Eq. 5** would reduce to the results solved by Esrig [23]. When both b and c equal zero, the solution of **Eq. 11** would be the same as the results proposed by Wan and Mitchell [24].

3. SOLUTIONS AND THEIR IMPLICATIONS

Based on the separation of variables method, the solution of **Eq. 5** for the boundary and initial conditions given in the above section is:

$$u = u_{\text{anode}}\frac{x}{L} + \sum_{n=0}^{\infty}\frac{1}{\left[\left(n+\frac{1}{2}\right)\pi\right]^2}\left\{16u_{\text{applied}}\left(\frac{1-(-1)^n\left(n+\frac{1}{2}\right)\pi}{\left(n+\frac{1}{2}\right)\pi}\right)+(-1)^n\left[8u_{\text{applied}}+2u_{\text{anode}}\right]\right\} \quad (11)$$
$$\sin\left[\left(n+\frac{1}{2}\right)\pi\frac{x}{L}\right]\exp\left[-\left(n+\frac{1}{2}\right)^2\pi^2 T_v\right]$$

where V_{anode} (V) is the electrical potential measured at the anode, T_v represents a dimensionless time factor, defined as $T_v = tc_v/L^2$. $u_{\text{anode}} = -\left(k_{\text{e}}/k_{\text{h}}\right)\gamma_{\text{w}}V_{\text{anode}}$ is the negative excess pore water pressure at the anode generated by electro-osmotic consolidation.

3.1 The average excess pore water pressure

The average value of excess pore water pressure u_{average}, which physically corresponds to the average excess pore water pressure for the entire cake thickness, is

$$u_{\text{average}} = \frac{\int_0^L u\,dx}{L} \quad (12)$$
$$= -\frac{u_{\text{anode}}}{2} + \sum_{n=1}^{\infty}\frac{1}{\left[\left(n+\frac{1}{2}\right)\pi\right]^3}\left\{16u_{\text{applied}}\left(\frac{1-(-1)^n\left(n+\frac{1}{2}\right)\pi}{\left(n+\frac{1}{2}\right)\pi}\right)+(-1)^n\left[8u_{\text{applied}}+2u_{\text{anode}}\right]\right\}\exp\left[-\left(n+\frac{1}{2}\right)^2\pi^2 T_v\right]$$

3.2 The average degree of consolidation

Wan and Mitchell [24] pointed out that for one-dimensional saturated soil electro-osmotic consolidation, the average degree of consolidation U_{average} (Pa) for the entire filter cake thickness at a given time t should be modified as:

$$U_{\text{average}} = \frac{\int_0^L\left(u_{\text{initial}}-u\right)dx}{\int_0^L\left(u_{\text{initial}}-u_{\text{final}}\right)dx} \quad (13)$$

where $u_{\text{final}} = u_{\text{anode}}\left(x/L\right)$ is the final excess pore water pressure, which can be obtained by applying $T_v \to \infty$ into **Eq. 11**. For the present initial condition, **Eq. 13** becomes

$$U_{\text{average}} = \frac{\frac{2}{3}-\frac{1}{2}\frac{u_{\text{anode}}}{u_{\text{applied}}}-\sum_{n=1}^{\infty}\frac{1}{\left[\left(n+\frac{1}{2}\right)\pi\right]^3}\left\{16\left(\frac{1-(-1)^n\left(n+\frac{1}{2}\right)\pi}{\left(n+\frac{1}{2}\right)\pi}\right)+(-1)^n\left[8-2\frac{u_{\text{anode}}}{u_{\text{applied}}}\right]\right\}\exp\left[-\left(n+\frac{1}{2}\right)^2\pi^2 T_v\right]}{\frac{2}{3}-\frac{1}{2}\frac{u_{\text{anode}}}{u_{\text{applied}}}} \quad (14)$$

3.3 The average porosity

The decrease in the filter cake thickness (*i.e.*, the compression of the filter cake) is equal to the change in the void ratio e, which can be calculated from the following equation:

$$H_{\text{initial}} - H = \int_0^L \left(e_{\text{initial}} - e\right) dx \tag{15}$$

where e_{initial} and e are the initial and instantaneous void distribution of the filter cake, respectively. Similarly, H_{initial} and H are the initial and instantaneous thickness of the filter cake, m, respectively. Furthermore, the average consolidation U_{average} can also be expressed as a change in the thickness of the filter cake:

$$U_{\text{average}} = \frac{H_{\text{initial}} - H}{H_{\text{initial}} - H_{\text{final}}} = \frac{\int_0^L \left(e_{\text{initial}} - e\right)}{\int_0^L \left(e_{\text{initial}} - e_{\infty}\right)} \tag{16}$$

where e_{∞} represents the critical void ratio defined by Iwata [17], at which electro-osmotic flow does not occur.

Integration of **Eq. 2** to t gives the change in local void ratio e during the time t.

$$e_{\text{initial}} - e = \alpha_v \int_0^t \frac{\partial u}{\partial t} dt = \alpha_v \sum_{n=1}^{\infty} \frac{1}{\left[\left(n+\frac{1}{2}\right)\pi\right]^2} \left\{ 16u_{\text{applied}} \left(\frac{1-(-1)^n \left(n+\frac{1}{2}\right)\pi}{\left(n+\frac{1}{2}\right)\pi} \right) + (-1)^n \left[8u_{\text{applied}} + 2u_{\text{anode}}\right] \right\} \tag{17}$$

$$\sin\left[\left(n+\frac{1}{2}\right)\pi\frac{x}{L}\right]\left(\exp\left[-\left(n+\frac{1}{2}\right)^2 \pi^2 T_v\right]-1\right)$$

If the initial void ratio e_{initial} distribution is known, then the void ratio distribution of the filter cake could be calculated based on **Eq. 17**. Furthermore, the average void ratio of the filter cake $\langle e \rangle$ at an arbitrary time could be obtained by integration of **Eq. 17** over the interval from $x = 0$ to L:

$$\begin{aligned} \langle e \rangle &= \langle e_{\text{initial}} \rangle - \int_0^L (e_{\text{initial}} - e) dx \\ &= \langle e_{\text{initial}} \rangle - \alpha_v \sum_{n=1}^{\infty} \frac{1}{\left[\left(n+\frac{1}{2}\right)\pi\right]^3} \left\{ 16u_{\text{applied}} \left(\frac{1-(-1)^n \left(n+\frac{1}{2}\right)\pi}{\left(n+\frac{1}{2}\right)\pi} \right) + (-1)^n \left[8u_{\text{applied}} + 2u_{\text{anode}}\right] \right\} \\ &\left(\exp\left[-\left(n+\frac{1}{2}\right)^2 \pi^2 T_v\right]-1\right) \end{aligned} \tag{18}$$

where $\langle e_{\text{initial}} \rangle$ is the average void ratio at the initial time. The average void ratio could be related to the average solids content $\langle w_c \rangle$ in w.t.% of the filter cake according to:

$$\langle w_c \rangle = \frac{100}{\left(\rho_w / \rho_s\right)\langle e \rangle + 1} \tag{19}$$

where ρ_s and ρ_w are the density of the solid particle and water, respectively, kg/m^3.

4. PARAMETER STUDY

According to **Eq. 11**, u_{applied}, k_e, k_h, and V_{anode} could have an impact on the electro-osmotic consolidation behavior. The variations of k_e, k_h and V_{anode} could be represented by u_{anode}. Therefore, the dimensionless ratio $u_{\text{anode}}/u_{\text{applied}}$ is used in the parameter study. Here we choose the cases of $u_{\text{anode}}/u_{\text{applied}}$ equaling to -0.5, -1.0, -2.0, and -4.0, respectively.

4.1 Excess pore water pressure development

The excess pore water pressure distribution as a function of the time factor T_v shown for different $u_{anode}/u_{applied}$ ratios is shown in **Fig. 2**. The dotted line in the figure represents the initial excess pore water pressure distribution in the filter cake. The results indicate that $u_{anode}/u_{applied}$ has a significant influence on the development of the excess pore water pressure in the filter cake. The greater the ratio of $u_{anode}/u_{applied}$ is, the faster the excess pore water pressure dissipates in the filter cake. Therefore, it indicates that increasing the voltage gradient could significantly promote filter cake consolidation or dewatering. At the same time, an excessively high voltage gradient would generate significant exothermic effects and increase energy consumption [25].

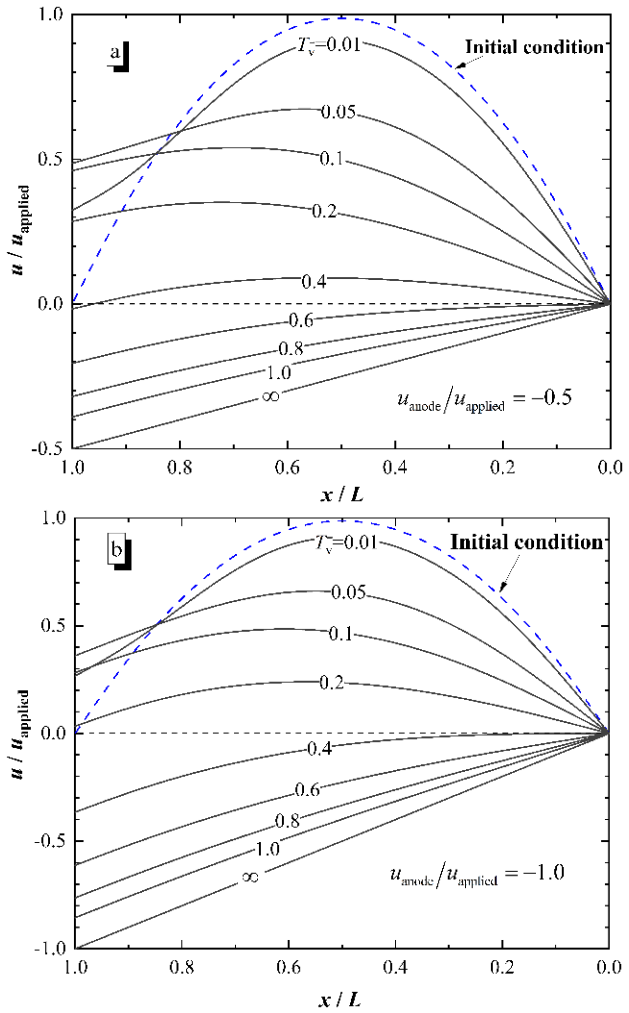

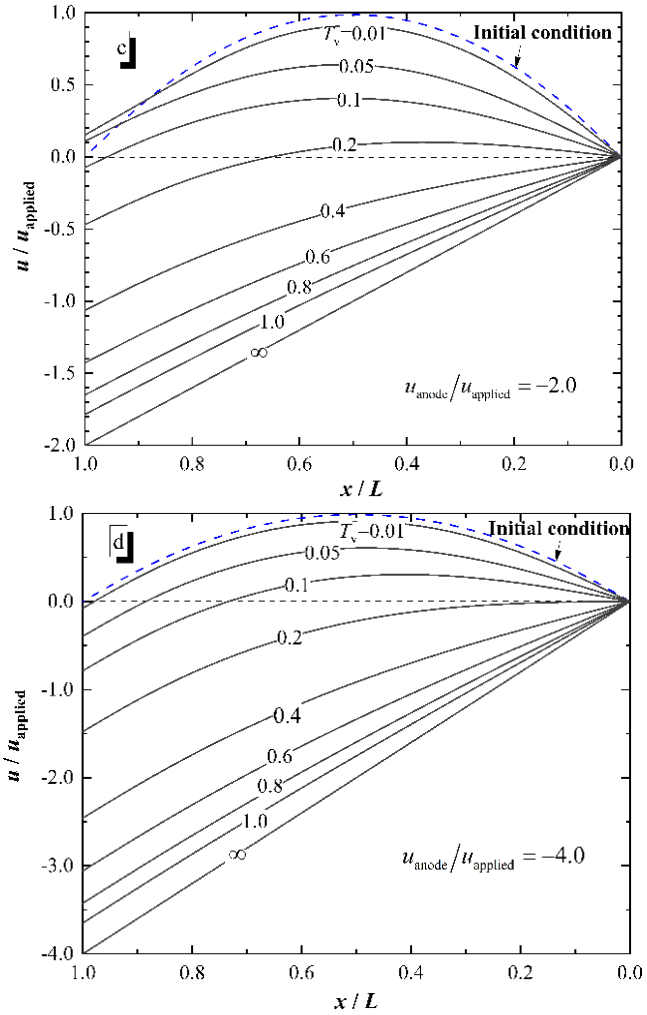

Figure 2. The excess pore water pressure distributions during the electro-osmosis consolidation with different ratios of $u_{anode}/u_{applied}$.

Interestingly, the excess pore water pressure in the region immediately adjacent to the anode (approximately between x/L = 0.8 and 1.0) increases in the beginning of the electro-osmosis consolidation when $u_{anode}/u_{applied}$ equals to -0.5, -1.0, and -2.0. The duration of this increasing trend decreases as $u_{anode}/u_{applied}$ increases (more negative). The reason for this phenomenon could be explained as follows. Since the anode is closed simultaneously as the electric potential is applied, the initial excess pore water pressure cannot dissipate through the drainage at the anode anymore, and an accumulation of energy will occur. When this accumulation is not sufficiently dissipated by the negative pore water pressure generated by electro-osmosis at the anode, the local pore water pressure will increase. While the negative pore water pressure caused by electro-osmosis at the anode is large enough to compensate for the initial pore water pressure, the pore water pressure increases at the anode at the beginning time after electro-osmosis will not happen (see **Fig. 2d**).

4.2 Average excess pore water pressure development

The development of average excess pore water pressure with different values of T_v based on **Eq.12** is shown in **Fig. 3**. Compared with the results when no electric field is applied ($u_{\text{anode}} / u_{\text{applied}} = 0$), the electro-osmotic drainage towards the cathode results in more rapid dissipation of the excess pore pressure caused by the initial filtration (see **Fig. 3a**). It could be observed that with the increase of the value $u_{\text{anode}} / u_{\text{applied}}$, the average excess pore water reaches zero at a small value of the time factor T_{v0}. The time required, T_{vo} , to dissipate the excess positive pore water is given in **Fig. 3b**. When the initial pore water pressure has a parabolic distribution, the value of the equivalent potential energy is about $0.67 u_{\text{applied}}$, which could be obtained by integrating **Eq. 9** over the interval from $x = 0$ to L . Although it is readily apparent that the superimposed electro-osmotic action significantly reduces the time required to dissipate a positive excess pore water pressure, the electrical energy consumed should also be considered. As can be seen, the relationship between T_{v0} and $u_{\text{anode}} / u_{\text{applied}}$ (**Fig. 3b**) is not proportional. When the absolute value of $u_{\text{anode}} / u_{\text{applied}}$ is greater than 0.5, the increase of u_{anode} does not lead to a significant reduction of T_{v0} . The results for a uniform distribution of the initial positive excess pore water provided by Wan and Mitchell [24] are also given in **Fig. 3b**. From the comparison results, the initial condition of pore water pressure with parabolic shape has a smaller T_{vo} with the same value of $u_{\text{anode}} / u_{\text{applied}}$. This implies that the former pressure with a parabolic distribution would dissipate faster than a uniform distribution when both have the same maximum value. From a practical point of view, the required duration of electro-osmosis would be overestimated if the initial condition was simplified to a uniform distribution.

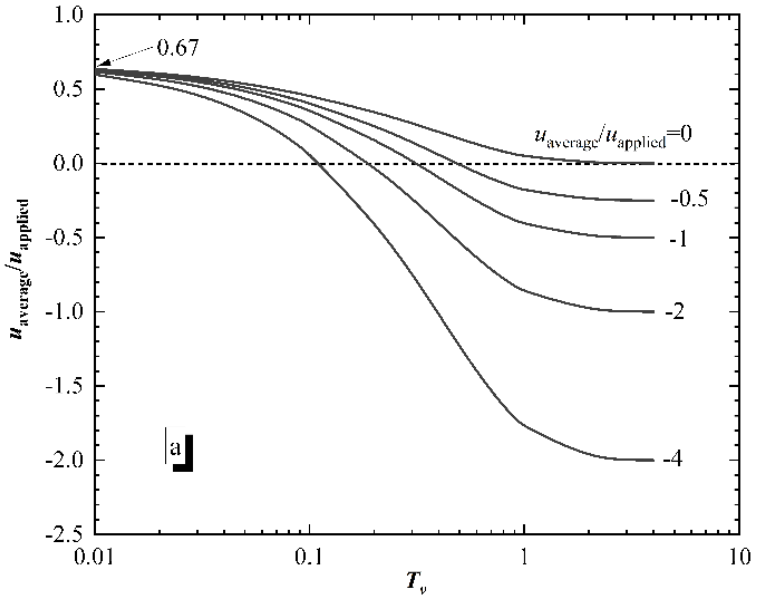

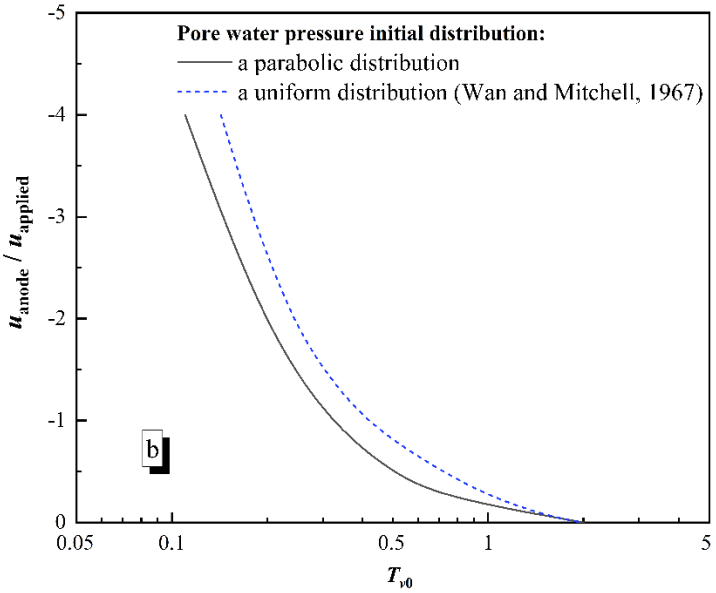

Figure 3. Average excess pore water pressure versus time factor during electro-osmotic consolidation.

5. EXPERIMENTAL VALIDATION

5.1 Materials and methods

Commercial washed kaolin produced in Jiangsu Province of China was selected as the model soil. The physical and chemical properties of the kaolin were listed in **Tab. 1**. The soil slurry was prepared by mixing the soil with de-aerated water to form a slurry with an initial water content of 3 times the liquid limit. Since the theoretical solutions are based on the assumption of constant k_h, k_e, and c_v, an over-consolidated sample should be prepared in the pre-tests. The feed pump used in the experiment could provide a maximum of 700 kPa pressure and a maximum 27 cm^3/s of flow rate. The total pressure on the filter cake was measured to be 600 kPa after the feed pump was turned off. Therefore, the slurry was pre-consolidated under 700 kPa by direct increment load to form a filter cake and rebounded to 600 kPa (*i.e.*, the over consolidation ratio = 1.17). Then the specimens were used for measurement of k_h, k_e, and α_v, respectively. The measurement of k_h was based on ASTM D5084 [26], and the test of k_e was based on the Shang and Mohamedelhassan [27]. The initial void ratio c_v was measured based on ASTM D2435 [28]. The results are listed in **Tab. 1**.

The experimental device used for validation is shown in **Fig. 4**. The acrylic cylinder with two end caps is designed to simulate one-dimensional electro-osmotic dewatering in the RCF press chamber. The prefabricated copper plate is used as the anode and cathode electrodes. The selected D.C. supply unit could provide a maximum of 30 volts output with a maximum current of 2 amperes. Since the negative pore pressures would be induced in the specimen, a back pressure system is designed to maintain positive pore water pressure during electro-osmotic consolidation for the convenience of pore water pressure measurement.

Table 1. Basic parameters of the model soil and the pre-consolidation specimen

Parameters	Value
Model soil	
Average particle size (μm)	50
Cation exchange capacity (CEC, cmol c/kg)	4.4
Plastic limit (wt%)	18.62
Liquid limit (wt%)	46.75
The density of the solid particles, ρ_s (g/cm^3)	2.65
Pre-consolidation specimen	
Initial void ratio $e_{initial}$	1.26
Hydraulic coefficient of permeability, k_h (cm/s)	1.95×10^{-7}
Electro-osmotic conductivity, k_e [cm^2·/(s·V)]	1.85×10^{-5}
Terzaghi coefficient of consolidation C_v (cm^2/s)	5.5×10^{-3}

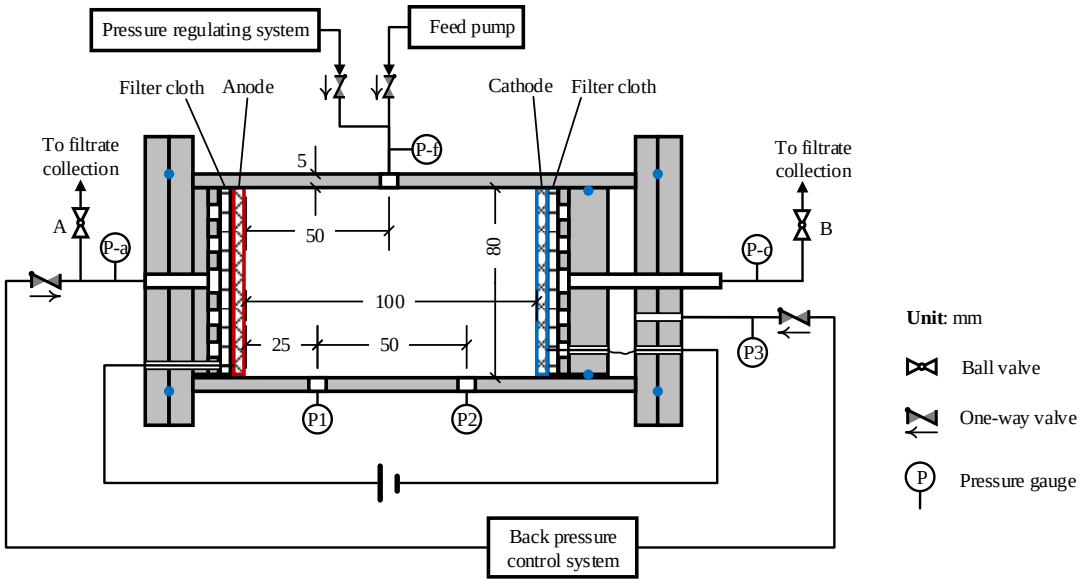

Figure 4. The schematic diagram of the experimental apparatus.

The prepared slurry is pumped into the cylinder by a feed pump with valves A and B open. When no filtrate is produced within 1 minute, the feed pump is closed and the pressure value of P-f is recorded as the $u_{applied}$. Then valves A and B are turned off, and the pressure regulating system and back pressure control system are turned on, whose pressure difference is adjusted equal to $u_{applied}$. After that valve B is open and the 20 V constant voltage of the power supply is applied to the anode and the cathode. For the present experiment, the value of $u_{applied}$ was 175 kPa, and the estimated maximum u_{anode} was 190 kPa based on the values of k_e and k_h listed in **Tab. 1**. Therefore, the back pressure of 250 kPa was sufficient to keep the pore water pressure in the specimen positive throughout the experiment. The duration of the experiment could be estimated according to T_v which is defined in **Eq. 11**. It could be calculated that the required time t was about 10 hours when $T_v = 2$.

5.2 The excess pore water pressure distribution

The excess pore water pressure values measured during the experiment were positive, from which the applied back pressure (*i.e.*, 250 kPa) should be subtracted to compare with the results according to **Eq. 11**. **Fig. 5** presents the calculated and experimental results of the excess pore water pressure. The calculated results show a good agreement with the experimental observations, especially when T_v = 0.2, 0.5, 1.0, and x/L is below 0.8. One of the most apparent differences between the observed and theoretical values occurs at the anode when $T_v = 2$. The reason for this discrepancy will be explained in the next section.

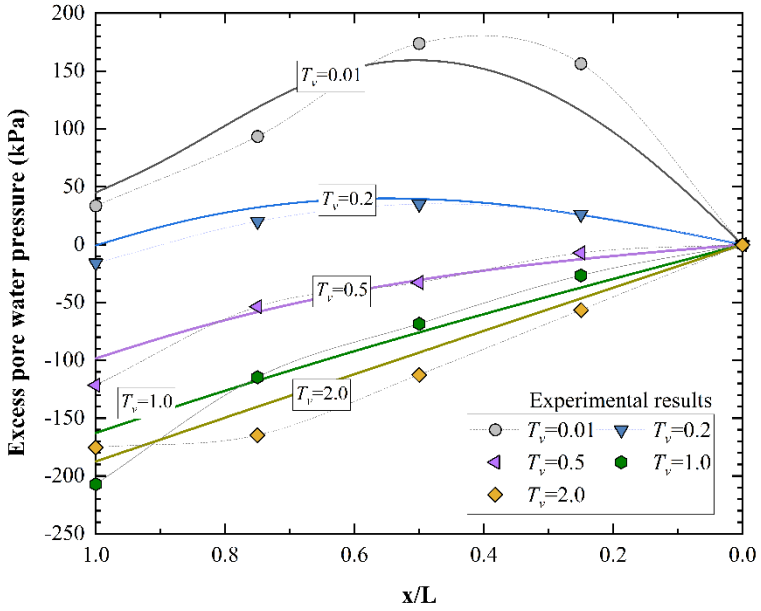

Figure 5. Pore water pressure distribution between anode and cathode at different times during electro-osmosis consolidation.

Meanwhile, it is also worth noting that the pore water pressure near the cathode increased a little during the initial stage (see the measured pore water pressure at $x/L = 0.25$ with $T_v = 0.01$). This temporary may be because the water flow towards the cathode was more significant than it could be drained in the early stage of the electro-osmotic dewatering [29]. As the water pressure was applied on the outside of the filter cloth, no initial increased pore water pressure was observed at the cathode. While from the significant increase in excess pore water pressure at $x/L = 0.25$ from the cathode, it could be inferred that the pore water pressure at the anode should be above zero when $T_v = 0.01$.

5.3 The excess pore water pressure measured at the anode

Fig. 6 provides the measured results and theoretical calculation of the development of pore water pressure at the anode. As expected, the excess pore water pressure experienced a gradual increase and reached the maximum value of 50 kPa at 10 min before it started to decline rapidly. The increase in the

excess pore water pressure in the first few minutes has been discussed in the previous section. The results reveal that the measured maximum pore water pressure was more negative than the theoretical solution. This discrepancy can be assigned to the hydraulic permeability coefficient (k_h) and the effective voltage (u_{anode}) variations during the electro-osmosis consolidation. It should be noted that the negative pore water pressure starts to decrease slowly (*i.e.*, less negative) if the electro-osmosis consolidation continues after the equilibrium point ($u = u_{anode}$) [30].

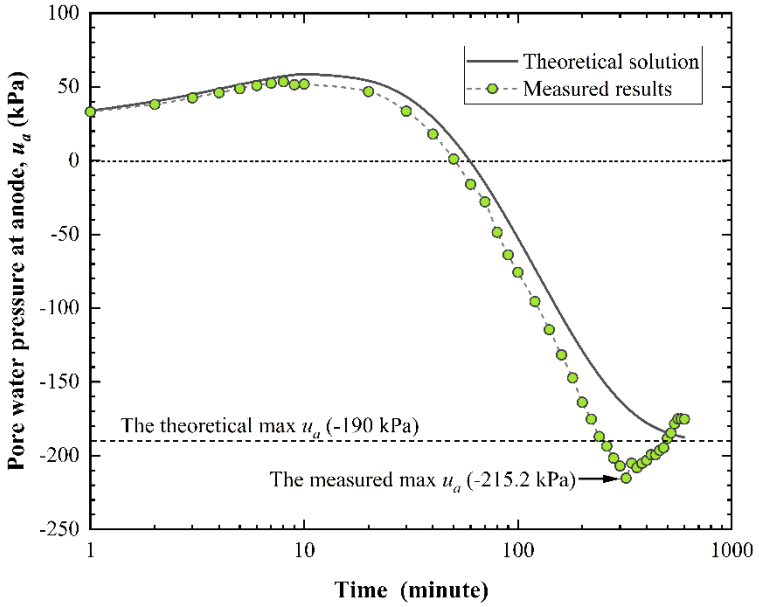

Figure 6. Variation of the pore water pressure at the anode with time during electro-osmosis consolidation.

5.4 Variation of the solid content

The measured solid content of the filter cake after different electro-osmosis consolidation periods is shown in **Fig. 7** and the solid line represents the predicted results calculated based on **Eq. 19**. Within 250 minutes ($T_v = 0.8$) of duration, the theoretical solution can well predict the experimental results, although the experimental observations are a little higher than the theoretical results. The back pressure application may explain this result in the experiment, which could generate a certain degree of compression effect on the specimen and the assumption of a uniform pore structure of the filter cake. Tiller and Horng [21] pointed out that both the porosity and the excess pore water pressure show a non-linear distribution along with the thickness of the filter cake. It should be noted that when $t > 360$ minutes ($T_v > 1.2$), the theoretical calculation has a distinct deviation from the experimental observations. As described in the previous section, the electrochemical effect in the filter cake will generate a significant impact if the electro-osmosis consolidation continues beyond the equilibrium state.

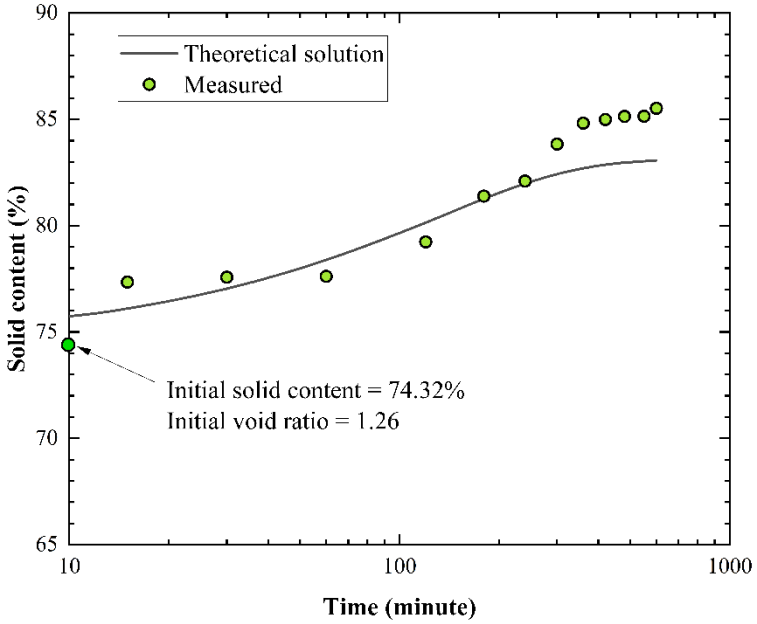

Figure 7. Comparison of the solid content over time between the theoretical calculation and experimental observation.

6 SUMMARY AND CONCLUSIONS

The following conclusions can be drawn from the present study:

(1) The proposed analytical results agree well with the experimental observations, which indicates the accuracy of the proposed analytical solution.

(2) The impact of the ratio of the negative pore water pressure at the anode to the maximum value of initial excess pore water pressure ($u_{\text{anode}}/u_{\text{applied}}$) was significant in the development of the electro-osmosis process. A more negative ratio would result in a quicker dissipation of the excess pore water pressure in the filter cake and a higher solid content.

(3) The initial excess pore water pressure existing within the filter cake with a parabolic distribution would increase the excess pore water pressure at the anode during the initial period of the electro-osmosis due to a change in the boundary condition. A more negative ratio would result in a shorter duration of the initial increased pore water pressure at the anode.

(4) The influence of the initial pore water pressure of the filter cake should be considered in predictions of the dewatering behavior of electro-osmosis in the RCF press.

ACKNOWLEDGEMENTS
We thank the Department of Educational of Liaoning Province for Key Laboratory (16-1077), the Discipline Innovation Team of Liaoning Technical University (LNTU20TD-11), and the National Natural Science Foundation of China (51874166) for the funding. We would also like to thank TopEdit (www.topeditsci.com) for its linguistic assistance during the preparation of this manuscript.

DISCLOSURE STATEMENT
No potential competing interest was declared by the authors.

References

1. J. Huazhe, W. Shufei, Y. Yixuan and C. Xinming. *J. Cleaner Prod.*, 245 (2020**)** 118882.
2. C. Wang, D. Harbottle, Q. Liu and Z. Xu. *Miner. Eng.*, 58 (2014**)** 113.
3. F. Shafaei, F.D. Ardejani, A. Bahroudi, M. Yavarzade and A. Amini. *Mine Water Environ.*, 40 (2021) 847.
4. M.T. Ammami, Y. Song, A. Benamar, F. Portet-Koltalo and H. Wang. *Electrochim. Acta.*, 353 (2020) 136462.
5. G.C.C. Yang, C. Min-Cong and Y. Chun-Fu. *Sep. Purif. Technol.*, 79 (2011) 177.
6. J. Zhou, Z. Liu, P. She and F. Ding. *Drying Technol.*, 19 (2001) 627.
7. H. Yukawa, H. Yoshida, K. Kobayashi and M. Hakoda. *J. Chem. Eng. Jpn.*, 11 (1978) 475.
8. W.A. Barton, S.A. Miller and C.J. Veal. *Drying Technol.*, 17 (1999) 497.
9. H. Saveyn, D. Curvers, L. Pel, P. De Bondt and P. Van der Meeren. *Water Res.*, 40 (2006) 2135.
10. M. Smollen and A. Kafaar. *Water Sci. Technol.*, 30 (1994) 159.
11. M.H.M. Raat, A.J.G. van Diemen, J. Lavèn and H.N. Stein. *Colloids Surf., A.*, 210 (2002) 231.
12. S. Hwang and K.S. Min. *J. Environ. Eng. Sci.*, 2 (2003) 149.
13. S. Kondoh and M. Hiraoka. *Water Sci. Technol.*, 22 (1990) 259.
14. B.K. Pandey and S. Rajesh. *Geotech. Geol. Eng.*, 37 (2019) 4649.
15. M. Iwata and M.S. Jami. *Drying Technol.*, 28 (2010) 881.
16. J.G. Sunderland. *J. Appl. Electrochem.*, 17 (1987) 1048.
17. M. Iwata, H. Igami, T. Murase and H. Yoshida. *J. Chem. Eng. Jpn.*, 24 (1991) 399.
18. M.S. Jami and M. Iwata. *Sep. Sci. Technol.*, 43 (2008) 979.
19. D. Curvers, K.C. Maes, H. Saveyn, B.D. Baets, S. Miller and P. Van der Meeren. *Chem. Eng. Sci.*, 62 (2007) 2267.
20. A.R. Dizon and M.E. Orazem. *Electrochim. Acta*, 304 (2019) 42.
21. F. M. Tiller and L.-L. Horng. *AIChE J.*, 29 (1983) 297.
22. M. Citeau, O. Larue and E. Vorobiev. *Sep. Sci. Technol.*, 47 (2012) 11.
23. M.I. Esrig. *Journal of the Soil Mechanics and Foundations Division*, 94 (1968) 899.
24. T.-Y. Wan and J.K. Mitchell. *Journal of the Geotechnical Engineering Division*, 102 (1976) 473.
25. Y. Shen, J. Feng, W. Shi and C. Qiu. *Int. J. Electrochem. Sci*., 14 (2019) 2136.
26. ASTM D5084, **2016**. Standard Test Methods for Measurement of Hydraulic Conductivity of Saturated Porous Materials Using a Flexible Wall Permeameter. ASTM International, West Conshohocken, PA.
27. J.Q. Shang and E. Mohamedelhassan. *ASCE Special Publication No. 112: Soft Ground Technology, ASCE*, Reston, VA, 2001, pp. 346–357.
28. ASTM D2435. 2011. Standard Test Methods for One-Dimensional Consolidation Properties of Soils Using Incremental Loading. ASTM International, West Conshohocken, PA.
29. L. Wang, Y. Wang, S. Liu, Z. Fu, C. Shen and W. Yuan. *Comput. Geotech.*, 105 (2019) 27.
30. I.R. Hamir. Some aspects and applications of electrically conductive geosynthetic materials. Ph.D. Dissertation, University of Newcastle upon Tyne, Newcastle , U.K., 1997.https://ethos.bl.uk/OrderDetails.do?uin=uk.bl.ethos.246694